

A statistical comparison of the AMIE derived and DMSP-SSIES observed high-latitude ionospheric electric field

E. A. Kihn,¹ R. Redmon,² A. J. Ridley,³ and M. R. Hairston⁴

Received 8 July 2005; revised 12 October 2005; accepted 1 December 2005; published 30 August 2006.

[1] The ion drift velocities and electric field derived from the Assimilative Mapping of Ionospheric Electrodynamics technique (AMIE) are compared with the same parameters observed by the Defense Meteorological Satellite Program's (DMSP) Special Sensor—Ions, Electrons, and Scintillation (SSIES) instrument. In addition the along-track cross polar cap potential, the correlation between the curves, and other metrics are compared and those results are binned by various criteria. The criteria include spacecraft, year, season, and magnetic activity level. We observed a reasonable correlation between the AMIE results and DMSP data with respect to the along-track potential, though the AMIE results tend to show a lower potential by some 30–50 percent, depending on spacecraft and orbit. Spacecraft in the same general orbits show similar relations with AMIE, implying that there is good intersatellite calibration for the DMSP array. There is a great deal of variability in the correlation, depending on season and activity level, and correlations with some of the spacecraft show a solar cycle dependence. It is further found that when we set a multifaceted criteria on each orbit for a DMSP-AMIE match, including along-track potential, V_y correlation, and peak potential locations, the results correspond between 35% and 55% for the dawn-dusk spacecraft, while they only correspond 7%–12% of the time for noon-midnight satellites.

Citation: Kihn, E. A., R. Redmon, A. J. Ridley, and M. R. Hairston (2006), A statistical comparison of the AMIE derived and DMSP-SSIES observed high-latitude ionospheric electric field, *J. Geophys. Res.*, *111*, A08303, doi:10.1029/2005JA011310.

1. Introduction

[2] The high-latitude ionospheric electrostatic potential field represents a basic signature of the interaction between the solar wind and the interplanetary magnetic field (IMF). It is now fairly well documented how the convection electric fields vary with changing IMF conditions, and a set of expected patterns have been derived for a wide range of solar wind and magnetospheric conditions. Maps of high-latitude convection electric fields are derived from numerous data and models. The models developed to describe these patterns can be broken down into a class of empirical models such as *Heppner and Maynard* [1987], *Rich and Hairston* [1994], *Papitashvili et al.* [1994], *Ridley et al.* [2000], and *Weimer* [1996, 2001] and data assimilation models such as *Kamide et al.* [1981] and *Richmond* [1992]. The empirical models are useful for describing the basic convection features and often have the advantage that

using the upstream IMF conditions they can be truly predictive as opposed to the nowcast/hindcast provided by the assimilative models. However, empirical models can only provide an “average” pattern for a given set of inputs and the actual pattern observed is likely to be different from the statistical *Bekerat et al.* [2003] in ways that carry operational impacts. Currently, the best approach for presenting a realistic modeled field is to use the assimilative models to ingest a comprehensive collection of observations while using statistical background models to fill in data gaps. The next step in the process is to understand how well the modeled output represents the observed environment. This type of study has been done for the Institute of Terrestrial Magnetism, Ionosphere and Radiowave Propagation electrodynamic model (IZMEM) in work such as *Dremukhina et al.* [1998] and *Kustov et al.* [1997]. In particular, *Kustov et al.* [1997] was able to show reasonable agreement between IZMEM and SuperDARN with respect to ion drift velocities for specific events. Taking this further, *Winglee et al.* [1997] intercompared AMIE, IZMEM, *Weimer* [1996], and a three-dimensional global simulation. They found that all four types of models show essentially the same features with respect to the auroral convection cells and were similar in their response in the cross polar cap potential with changing solar wind conditions. A body of work similar to this study was done by *Papitashvili et al.* [1999] and *Papitashvili and Rich* [2002] for the IZMEM

¹National Geophysical Data Center, NOAA, Boulder, Colorado, USA.

²Center for Investigatory Research in Environmental Sciences, University of Colorado, Boulder, Colorado, USA.

³Center for Space Environment Modeling, University of Michigan, Ann Arbor, Michigan, USA.

⁴William B. Hanson Center for Space Sciences, University of Texas at Dallas, Richardson, Texas, USA.

model; however, they were using Defense Meteorological Satellite Program (DMSP) observations to calibrate the model rather than a strict intercomparison of the results. With respect to AMIE several studies have focused on the performance of the AMIE model over specific intervals [Lu *et al.*, 1996], but very little work has been done comparing the performance over extended periods [Kihn and Ridley, 2005]. We believe this is a significant oversight for a model used extensively in the scientific community.

[3] We present the results of a multiyear comparison between AMIE model output and DMSP satellite observations of ion cross track velocity. A quantification of the errors in AMIE and possible errors in DMSP measurements is presented. These results can be used to evaluate AMIE as a tool for operations and where the AMIE outputs are being linked to other models.

2. Data Description

[4] This section contains brief descriptions of the AMIE archive employed in the evaluation, the DMSP Special Sensor–Ions, Electrons, and Scintillation (SSIES) instrument, and of the filtering required to use that data for comparison.

2.1. AMIE

[5] The AMIE output used in this project was created as part of the Space Weather Analysis (SWA) program at the National Geophysical Data Center. The SWA project is an attempt to link several data driven models with historical archives to create a complete 11-year record of the near-Earth space environment. The SWA used 11 years (1992 to 2002) of cleaned and quality-controlled global magnetometer data, as well as the available IMF, solar wind, HPI, $F_{10.7}$, and D_{st} data to produce an archive of AMIE runs at 1-min resolution [Ridley and Kihn, 2004]. The reasoning behind using these inputs for the period is that the data availability across the period is quite stable for these particular input parameters meaning there is less chance of a bias due to inconsistent observations. Because of the uneven station coverage between hemispheres, we have chosen to compare only the northern hemisphere (which has more complete data coverage) AMIE outputs with DMSP. The northern hemisphere ground station data available in this period is very stable and approximately 90 high-latitude and midlatitude stations were used in the calculation of the electric potential pattern presented here. It is worth noting that in this study we are using AMIE runs that were completed using a minimal and commonly available set of input data that more closely matches the operational environment than a postevent research run.

[6] Restricting our study to AMIE driven primarily by magnetometers imposes a limit on the scope of the study. However, when using magnetometers to determine the potential pattern, we do derive some advantages: (1) magnetometers offer a consistency in location of measurement that many other techniques (such as in situ satellite and SuperDARN radar measurements) do not offer; (2) Sun-synchronous satellite measurements sample only a cut through the pattern, while magnetometers offer a semiglobal view of the convection pattern all day, every day; (3) this technique allows a determination of the global electric

potential for many years on a 1-min timescale, which cannot be done by any other technique with nearly the same global-scale coverage; and (4) because there are magnetometer stations available in near-real-time and since AMIE can be run using solely the ground magnetic disturbance data, this mode of operation has an impact on operational evaluation of the model.

[7] Using the data as described above, we applied no further filters, transforms, or modifications to the archive and used the data directly for comparison with DMSP SSIES.

2.2. DMSP SSIES

[8] An observational comparison was made using the Defense Meteorological Satellite Program's (DMSP) satellites. The DMSP spacecraft carry an array of space environmental sensors that record along-track plasma densities, velocities, composition, and drifts [Rich and Hairston, 1994].

[9] For independent comparison with the AMIE results described above, we use the ion drift meter (IDM) data, which is a subcomponent of the SSIES carried on the DMSP satellites starting with F-8 in June 1987 [Rich and Hairston, 1994]. The IDM measures the horizontal and vertical angles of arrival of ions with a 6 Hz sample rate (we are using 4-s binned averages derived from this), and given this angle and the known speed of the spacecraft, the particle cross-track speeds can be deduced. We indirectly make use of the retarding potential analyzer (RPA) which can determine the total ion density and ratio of O⁺ to H⁺ or He⁺, among other parameters. The O⁺ ratio is required because when H⁺ or He⁺ represent more than 20% of the ambient plasma the IDM measurements are affected and considered bad. This is more often observed near solar minimum and in the winter hemisphere. We also remove the corotation component of the cross-track velocity from the DMSP observations because the AMIE patterns are derived in a rotating coordinate system, while DMSP is measuring the corotation velocity.

[10] In order to convert the DMSP measured cross-track flows to a convection electric field (\mathbf{E}), the topside ionosphere is assumed to be a collisionless plasma. Then given that

$$\vec{E} = -\vec{V} \times \vec{B} \quad (1)$$

and that DMSP measures V_y (where x is along the satellite path and z is radially away from the center of the Earth), $\vec{E}_x = -V_y B_z + V_z B_y$. We neglect V_z and B_y , since they are significantly smaller than B_z and V_y in the polar region, meaning that $E_x \cong -V_y B_z$. In this paper we are using the IGRF as our \mathbf{B} field. In addition to ion velocity, we are interested in computing the along-track electrostatic potential, derived by integrating the DMSP observed electric field along the spacecraft track. To do this, it is assumed that at some latitude, the potential drops to zero. In our case we chose 50° as the zero boundary on the ascending part of the orbit. We then check that on the descending crossing of 50° that the calculated potential returns to zero. The case is which it fails to return is described in the next section.

[11] In this study we were fortunate to have multiple years of data available both from AMIE and DMSP. This

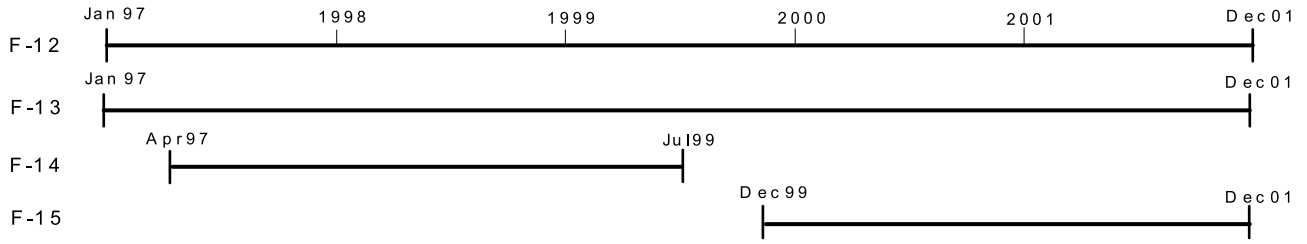


Figure 1. The DMSP SSIES data range used in this study.

allows us to perform our comparisons across multiple years, seasons, and solar conditions. Specifically, SSIES data from the spacecraft as listed in Figure 1 is used over the 5-year period. This amounts to over 70,000 potential comparisons; however, that number was greatly reduced by filtering on the SSIES data as described in the following section.

2.3. Data Filters

[12] As is typical for a scientific data set, there are several filters that must be applied when using the IDM data for comparison. The first filter we applied is that on a particular orbit at least 70% of the data above 50° is labeled good. All of the IDM data are quality flagged either as good, bad, caution, or unknown based on the RPA values. If we do not have at least 70% good data in the region of interest, the orbit is excluded. We also require that there be greater than 100 data points above 50° in the northern hemisphere to assure a reasonable number of comparison points or we exclude the orbit. Next, we allow a maximum of 3 min between good data points in the auroral zone or the orbit is excluded. We check the SSIES data for several time parameters including that time is always increasing, that there are no out of range time values for the orbit, and that IDM times provide a reasonable split between duskside and dawnside values. Finally, we calculate the along-track cross polar cap potential for each orbit and require that the calculated end value for the potential be within the range $0 \pm 25\%$ of the observed maximum for the orbit. There are several possible reasons why this might occur including sunlight contamination of the IDM, the presence of a penetration electric field, a rapidly varying convection pattern, or expansion of the auroral oval to latitudes lower than 50° . Given the large amount of data, it is outside the scope of this study to check each case, so orbits that fail to return to zero (within 25% of maximum potential) are discarded as bad. After all these filters have been applied, a significant number of comparison points remain as shown in Figure 2. This figure further illustrates that the DMSP coverage is primarily in the 0600–2000 MLT sectors with gaps around 1200–1500 MLT and 2200–0400. The uneven coverage could bias the results by over sampling the dusk potential cell and missing entire components of the dawnside but is unfortunately unavoidable.

3. Comparison Techniques

[13] Every orbit of DMSP IDM data that passes the filtering described in the previous section is compared with the archived AMIE data. A sample comparison is shown in Figure 3. We are comparing the AMIE output and IDM data averaged to 1.0 min and evaluating three primary quantities:

(1) along-track polar cap potential (AT-PCP), (2) the magnitudes of V_j , and (3) the general shape of the patterns. First, we convert the IDM measured V_y to electric field using equation (1), then integrate along the orbital track from 50° to 50° to get an AT-PCP from both AMIE and the IDM. For the IDM data, we linearly adjust the values so that the end points correspond to a zero potential. In the AMIE case, for each time step, we take the closest data file in time and interpolate in space to the spacecraft location. The potential pattern shown as part of Figure 3 is taken from the time nearest the midpoint of the pass, but the comparison data does vary in time.

[14] Next, we are interested in how the curves correspond in shape. For that metric we could have chosen to use the cross-correlation coefficient, but instead we choose to present the normalized mean square error. Normalized mean square error (NMSE) comes from the field of neural forecast modeling and was introduced by *Casdagli* [1989] for cross-comparison of the quality of a predictor for different output signals and time windows. NMSE is defined as

$$NMSE(N) = \frac{1}{\sigma_T^2 \cdot N} \sum_{k \in T} (x_k - \hat{x}_k)^2, \quad (2)$$

where x_k is the true value, \hat{x} is its prediction, T is the test data containing N points, and σ_T^2 is its variance.

[15] In our case, the DMSP observation is taken as x_k , the AMIE prediction is taken as \hat{x}_k , and the summation is over the set of points in a given orbit. The advantage of NMSE over cross-correlation is that it is intended as a measure of the information content between signals and we can more easily assign a value that represents an acceptable correlation. The NMSE also has the advantage that a value of 1.0 or higher implies no information content between signals and therefore serves as a reference boundary.

[16] In addition to the three primary comparisons described above, we record for each orbit, for both AMIE and the DMSP data the maximum and minimum potential, the location of the maximum and minimum, and the cross correlation coefficients on the dawnside and duskside orbits. The resulting statistics are binned by activity level, spacecraft, time of year, and season.

4. Results

[17] The results are binned according to different criteria and we identify the significant trends detected. The first set of the results are those shown in Figure 4. The interesting elements to note from these plots are that (1) for all of the spacecraft the AMIE values of AT-PCP tend to be lower

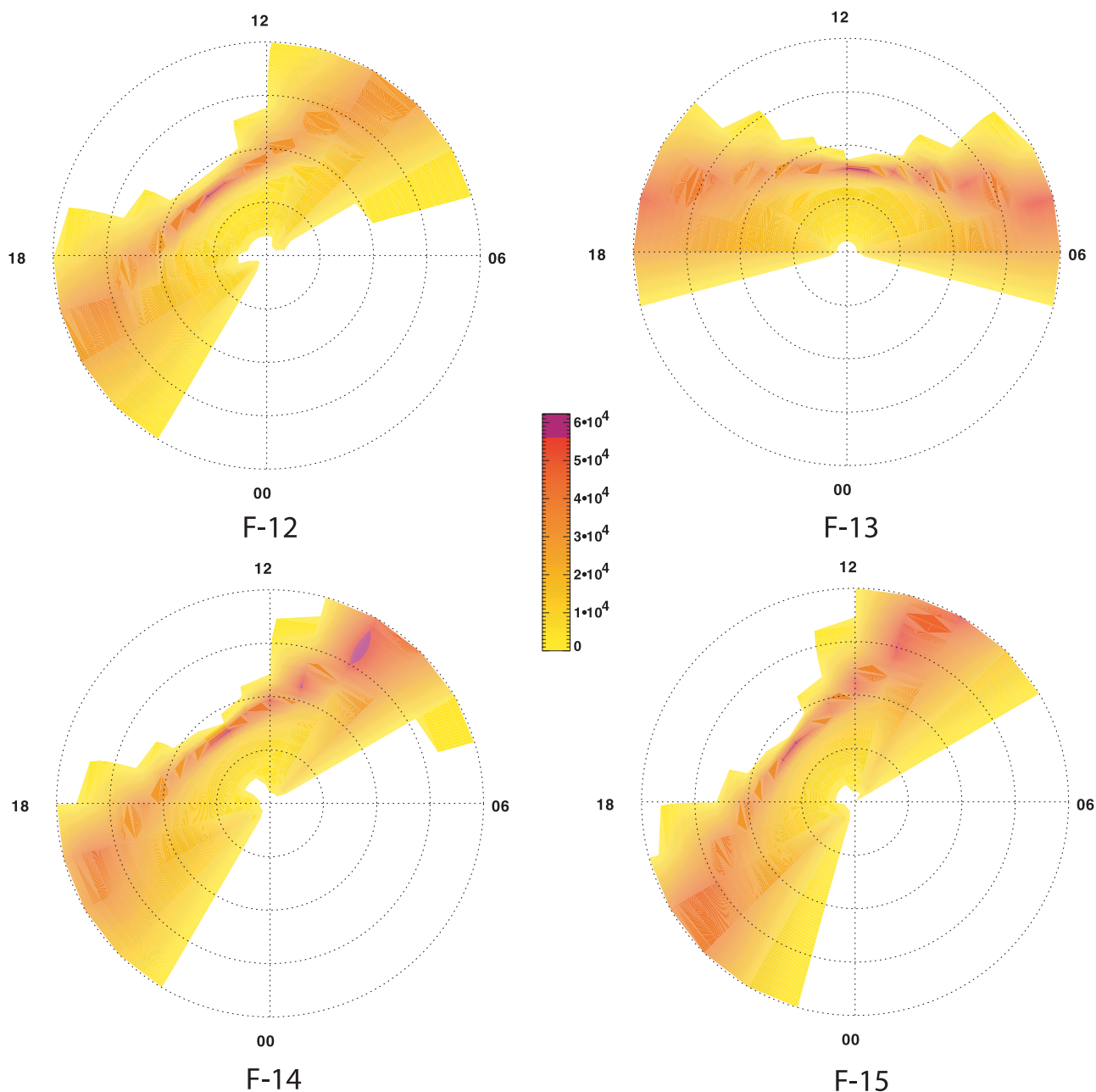


Figure 2. This plot shows the frequency of DMSP observation in a given AMIE grid cell. The values are for the data which has passed all the quality filters and not every orbit.

than DMSP observations, (2) the satellites in the “noon-midnight” orbits all have similar AT-PCP trends and they are much lower than the F-13 result, (3) despite having a much longer observing period, F-12 has relatively few data points left after filtering. In several of the other results in this section we observed that the “noon-midnight” satellites display common characteristics with respect to each other, but not necessarily to F-13.

[18] Next, we were interested in any solar cycle effect and binned the data by year to derive the results in Figures 5 and 6. It is interesting to note here that (1) the correlation for F-13 is nearly unchanged from year to year, (2) the correlation for F-12 improves significantly from year to year, (3) the 1997 data from F-12 had virtually no orbits

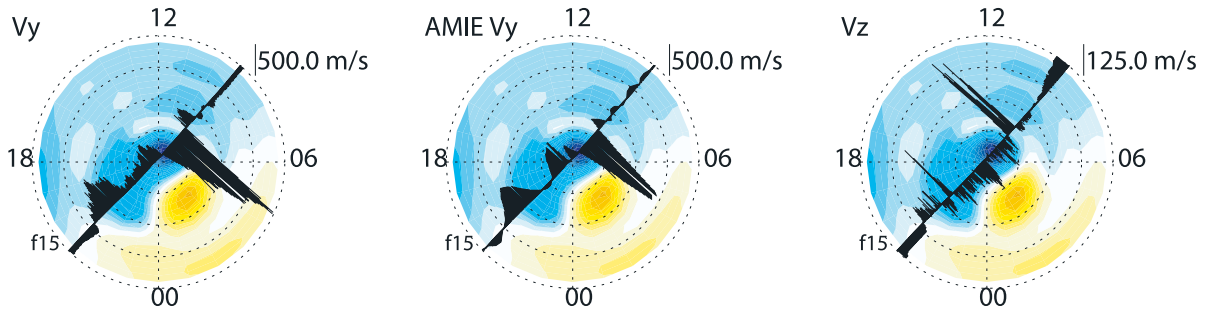
which passed our check criteria, and those few which did seemed almost random with respect to the AMIE result.

[19] Here we note that both F-14 and F-15 showed the same trend as F-12, though they are not shown in a figure.

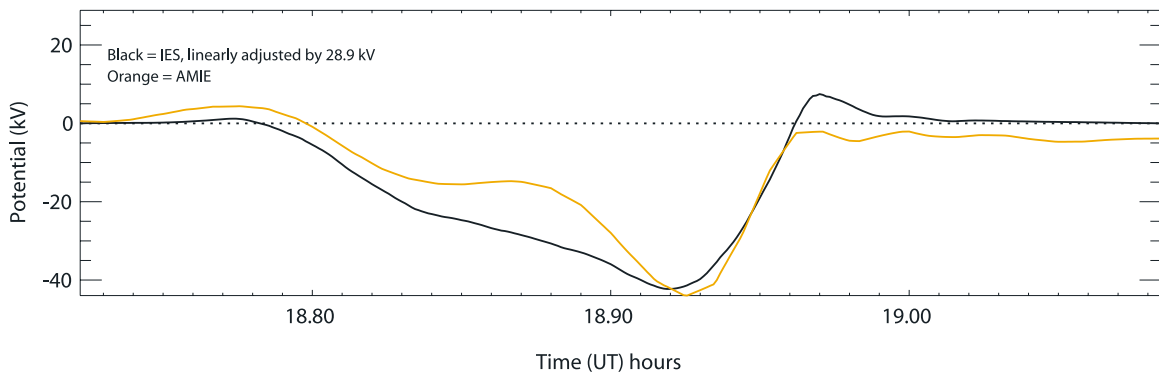
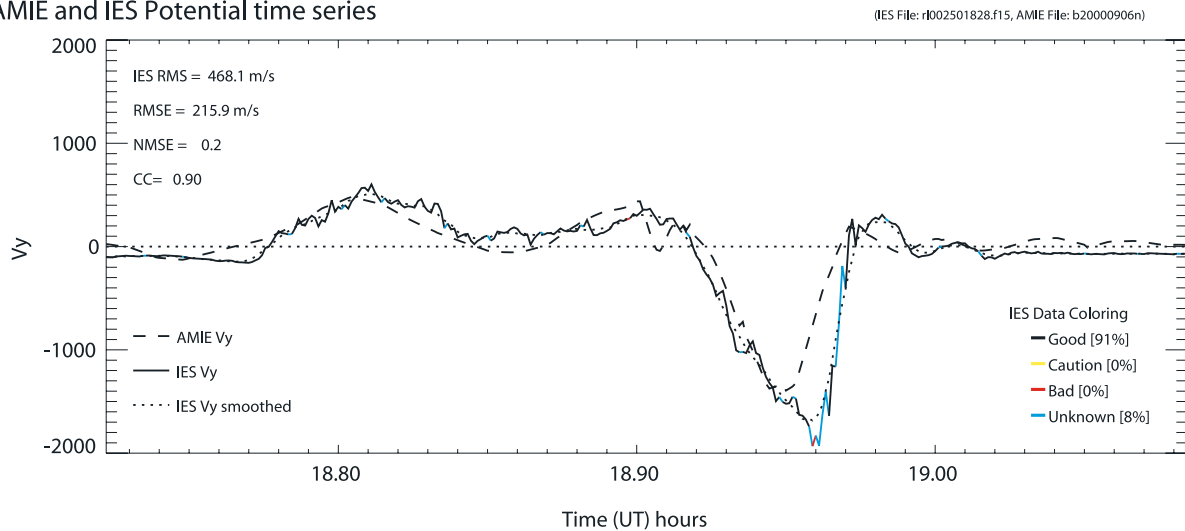
[20] Subsequently, we looked for seasonal effects in the data, taking both summer and winter to be the appropriate northern hemisphere seasons corresponding to our area of study. Figure 7 shows a clear difference in the AT-PCP ratio between the summer and winter data for all satellites. We attribute this result primarily to a problem with the AMIE minimum winter conductance; this is covered further in the discussion section.

[21] When looking at the activity level correlation, using AL as a measure, we see in Figure 8 that there is a slight

AMIE Potential Contours over IES Velocities



AMIE and IES Potential time series



Info: 2000-09-06

%IES Data Used = 100%

CPCP (IES): 55.1 kV, min=-26.6, max= 28.9

CPCP (AMIE): 48.3 kV, min=-44.0, max= 4.4

Cross Correlation (Vy): 0.90, max=0.951 (at Lag=-20.0 sec)

Dusk: 0.84, max=0.855 (at Lag=-12.0 sec)

Dawn: 0.89, max=0.936 (at Lag=-16.0 sec)

Figure 3. A plot showing a typical comparison between the AMIE output and DMSP observations. The top row is a plot of DMSP V_y , AMIE V_y , and DMSP V_z (black) over the AMIE potential. The spacecraft ID label marks the start of the orbit. The second panel is the DMSP V_y (solid) versus the AMIE calculated (dashed) with a color coding for the DMSP quality flags. The bottom panel shows a running potential IES (black) versus AMIE (orange) AT-PCP calculated from the respective V_y s.

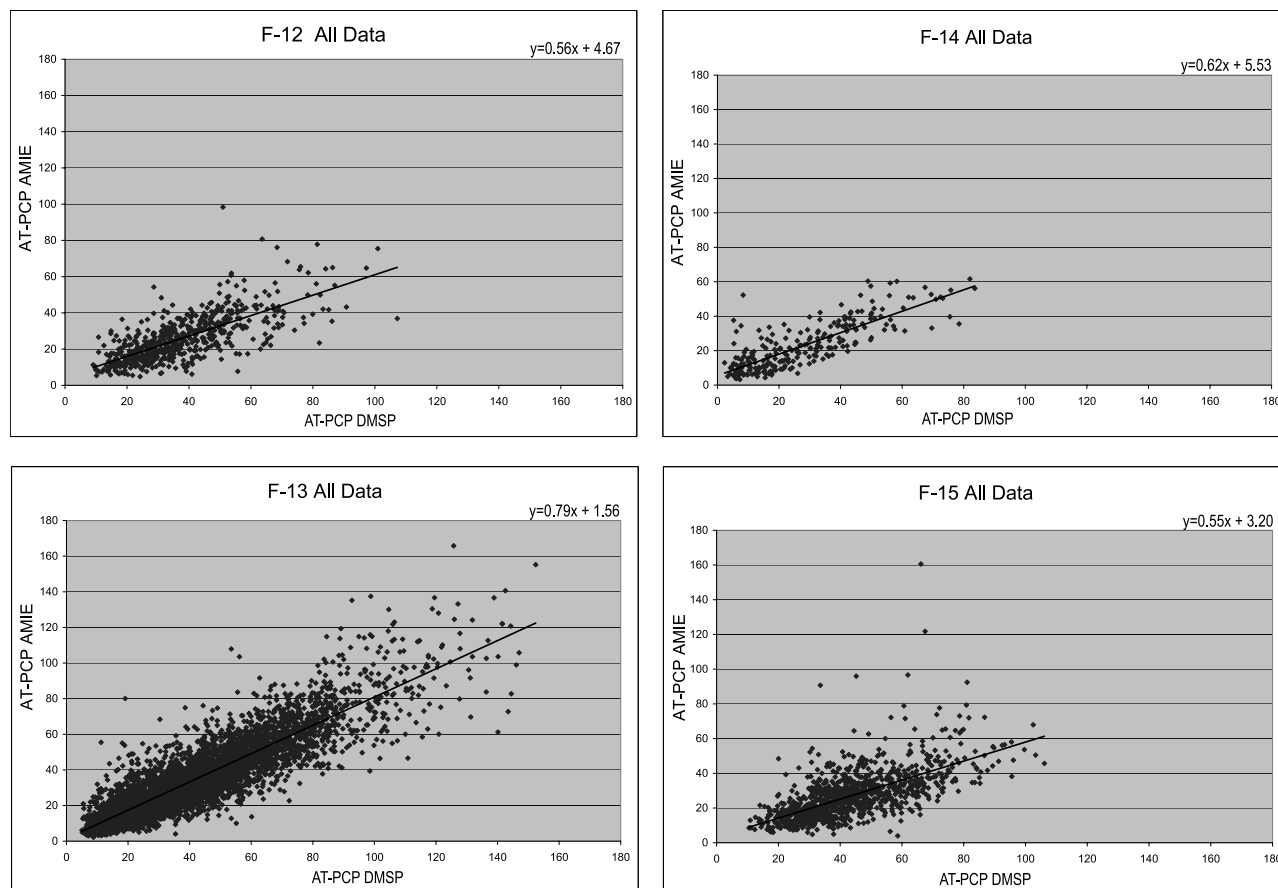


Figure 4. A plot of the along-track polar cap potential as observed by DMSP and calculated from the AMIE results. The data are for the full time range used in the study and all orbits which passed our criteria as described in the data description section.

trend toward better correlation with AT-PCP magnitude with increasing activity level for F-13. However, the plot also shows an increased scatter across activity levels so the individual orbits may be less well coupled. Interestingly, the other spacecraft show differing trends, with F-12's AT-PCP becoming less well correlated with increasing activity, while F-14 and F-15 both correlate slightly better.

[22] Finally, we used the $NMSE-V_y$ calculated on the entire sample to calculate the percentages in Table 1. It is interesting to note that despite the difference in the AT-PCP calculations between satellites the NMSE scores are fairly similar. The exception being F-14 which is 60% of the time virtually uncorrelated with the AMIE data.

[23] While these statistical summaries give a feel for the correlation of model and observation, they do not give a sense of how well one might expect the two to correlate from orbit to orbit as might be needed in an operational setting. For that we follow the style of *Bekerat et al.* [2003] and define a set of criteria for a matching orbit. Specifically, we define a successful match as (1) the AMIE calculated along-track polar cap potential is within 50% of the SSIES value, (2) the minimum and maximum potentials are within two degrees MLAT of each other, and (3) the NMSE for the orbit is less than 0.5.

[24] There are significant differences between the *Bekerat et al.* [2003] criteria used to evaluate the *Weimer* [2001] model and our results. For example our filtering criteria

eliminates over 60% of the F-13 orbits from consideration based on runaway potentials, whereas *Bekerat et al.* [2003] used these. We vary our AMIE pattern in time with the orbit where *Bekerat et al.* [2003] used a fixed time for comparison and varied the input parameters. We believe these are significant issues which should be considered when using the result. The results of our comparison are summarized in Table 2.

[25] The next section provides comments on each of the trends observed in the study.

5. Discussion

[26] As we presented in the introduction section, this paper is meant as an intercomparison between two different data sets and not as an absolute validation of either. Of course when the two independent observations agree, it promotes confidence in both. In the preceding sections we have seen that in this case the two have some significant differences. Where there is an important difference, ideally we would turn to a third data source and use that as an arbiter. So, though we do not answer in an absolute sense the question of which observation or model output is correct, we do derive some interesting results on their own. For example, when considering the three satellites in the noon-midnight orbit, we can observe using AMIE as the comparison basis between the three that they are reasonably

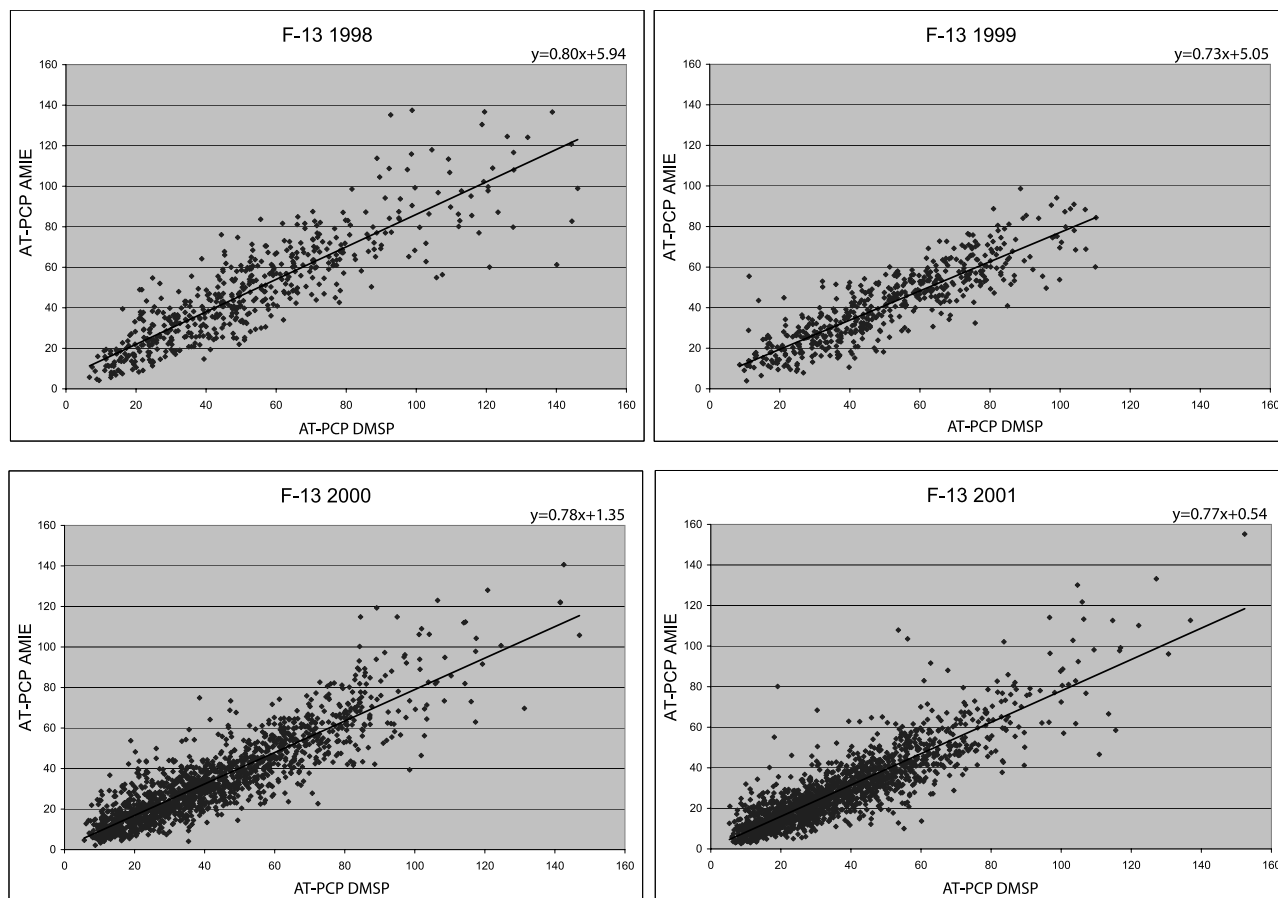


Figure 5. A plot as in Figure 4. The data are binned by year for F-13. Notice there appears to be no significant yearly trend in the F-13 data.

well calibrated. The spacecraft have nearly identical relations to AMIE with respect to AT-PCP and respond very similarly with respect to changing year and season as well. Clearly, it is of interest that the F-13 spacecraft compares quite differently to AMIE than the others. Unfortunately, we do not have access to another spacecraft in this orbit to see if it is a function of the orbit, the instrument itself, or possibly some property of the AMIE model in the given MLTs. Looking first at DMSP, we see one possible explanation in the northern polar regions for the F12, F14, and F15 data. The IDM data from these three spacecraft show anomalous high-speed horizontal sunward flows at certain times of the season and solar cycle in the northern polar region that we

do not believe are real. Because of the orientation of the IDM’s aperture to the Sun angle in this orbit, it is possible the Sun is hitting at just the right angle as the spacecraft comes over the north polar region (heading sunward) to light up one of the edges of the IDM (that is behind all the suppressor grids. This would cause photoemissive electrons to be produced inside the IDM just above the collectors. The repellers grids that are supposed to keep the outside electrons from entering the IDM would then keep these photoemissive electrons in. Such electrons then end up on the collectors and give an erroneous current reading that makes it appear there is an excess cross-track flow. In the case of these three satellites where the IDM faces sunward as the

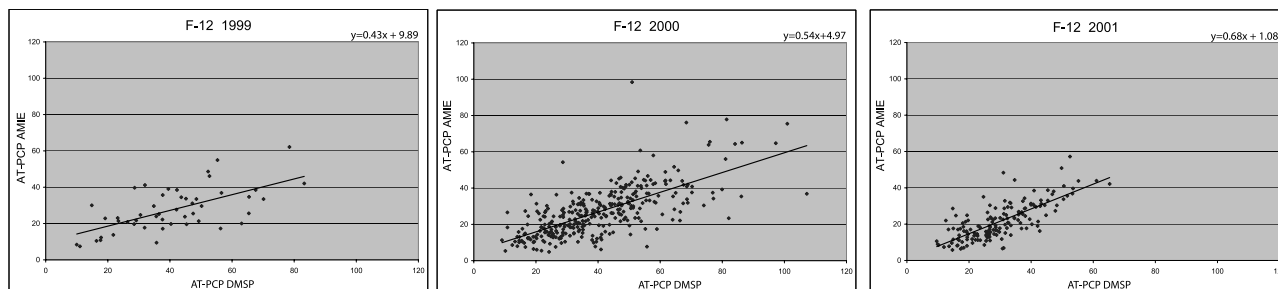


Figure 6. A plot as in Figure 4. The data are binned by year for F-12. Notice the improving AT-PCP ratio and decreased scatter between AMIE and F-12 as the data approach solar maximum.

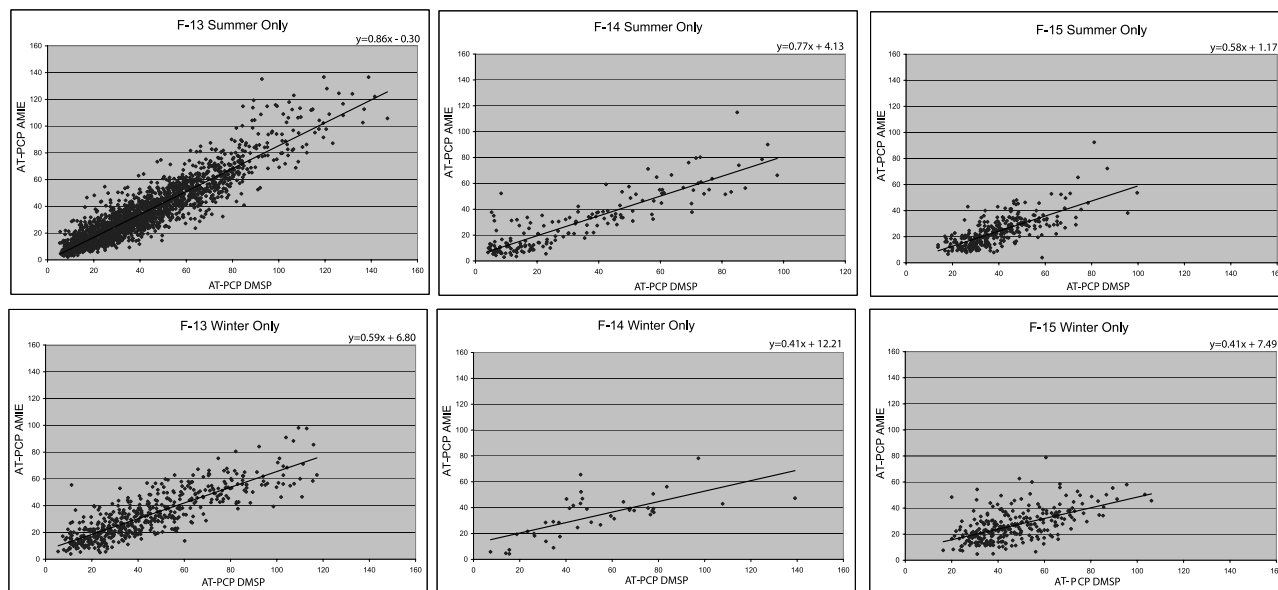


Figure 7. A plot as in Figure 4. The data are binned by satellite and season. There is a clear difference between the summer and winter correlations for all satellites.

spacecraft comes up over the dusk-to-midnight quadrant of the northern polar region heading toward the dawn-to-noon quadrant, the sunlight hits the right inside edge (when looking out of the IDM in the direction of the spacecraft's velocity vector), so the electrons hit the right-side collectors primarily. Because of the negative sign of the electron current, this gets read as excess positive current on the left-side collectors and the IDM reports a large cross-track flow to the left (+y or roughly sunward side). This explanation for an excess +y ion flow for a short period on this sunward leg matches the observations seen on F12, F14, and F15. This anomaly in these three spacecraft is more pronounced in the winter than summer and disappeared as we approached solar maximum conditions; in other words, the anomalous flows disappeared as the average plasma density increased. Since the amount of current from the photoemissive electrons is roughly constant over the solar cycle, once the current from the ions becomes large enough to dominate the electron current, the horizontal IDM flow data would return to normal. It should be emphasized that this is only our working hypothesis to explain this anomaly and that no direct test of this idea has been attempted yet. Of course since we have filtered all the orbits in which the cross polar cap potential fails to return to zero, in theory we

should not see this effect, but it may be a lingering bias in all the data driving the potential higher. The best evidence for this perhaps comes from the yearly changes in AT-PCP for the spacecraft in the noon-midnight orbits. While there is little or no change in the F-13 data, the others show better correlation with AMIE, perhaps as the percentage contribution from the light contamination decreases.

[27] Another possibility for the discrepancy between F-13 and the other spacecraft is that the along-track velocity (V_x) of the ions is neglected in the processing of the IDM data. Typically, the correction for this is small because of the low ratio of the ion velocity to the spacecrafts own ≈ 7.5 km/s velocity. However, it is possible that because the F-13 orbit cuts through the dusk convection cell more perpendicularly than the other spacecraft, thereby minimizing V_x , that there is less error introduced. However, even in a worst-case scenario this cannot account for the full difference observed.

[28] Of course, DMSP instrumentation is unlikely to be the only cause of the difference. A spacecraft in a noon-midnight orbit has the possibility to come up the boundary between the dusk and dawn convection cells. In this case, if the AMIE pattern is slightly rotated from the actual pattern, then the model may be giving near-zero fields, when in fact, there are reasonably large fields present. In part, this points

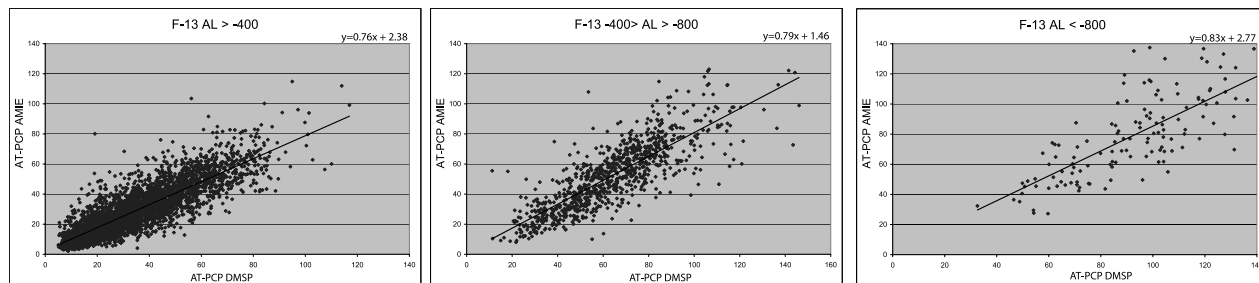


Figure 8. A plot as in Figure 4. The data are binned by the minimum AL calculated by AMIE during the time of the DMSP pass.

Table 1. Percentage of DMSP Orbits Which Match the AMIE Data According to the Specified NMSE Criteria^a

| Satellite | NMSE < 0.5 | 0.5 < NMSE < 1.0 | NMSE > 1 |
|-----------|------------|------------------|----------|
| F-12 | 38.3% | 37.0% | 24.7% |
| F-13 | 43.3% | 30.7% | 26.0% |
| F-14 | 10.6% | 28.6% | 60.8% |
| F-15 | 34.7% | 46.7% | 18.6% |

^aThe result is for all samples which passed the specified filtering.

out the problem with taking a line sample of spatial output but is the best possible approach with the currently available data resources. Since the F-13 orbit is sampling more through the “heart” of the pattern, a slight rotation has a far less dramatic effect on the final potential leading to better correlation with the observation. It could also be that something in the background conductance model is off for these particular MLTs. The background models used in these AMIE runs [Ahn *et al.*, 1998; Fuller-Rowell and Evans, 1987] were shown by Kihn and Ridley [2005] to be quite low with respect to DMSP Precipitating Electron and Ion Spectrometer (SSJ/4) observations for example. In this case, that makes matters worse because too low a conductance implies too high a potential. This type of effect, where a background model which strongly drives the AMIE result is poorly calibrated, is illustrative of the potential for error in AMIE. Of course, as AMIE is a data assimilation model when improved background models become available they can be simply plugged in to get an improved result.

[29] With regard to the seasonal variations, we see in Table 3 that our results correspond with those of Papitashvili and Rich [2002] quite well. That is to say, for both F-12 and F-13 we see a relatively flat AT-PCP with a 10% enhancement in the winter. Conversely, with AMIE we see a flat AT-PCP with a 10% decrease in the winter. The Papitashvili and Rich [2002] result is more consistent with de la Beaujardiere *et al.* [1991], which leads us to suspect a problem with AMIE. We suspect the AMIE mode’s minimum value for conductance of 2 mhos is too high. If this value were too high for the winter data, it would show up as too low a potential. We are unaware of any published value for appropriate minimum winter conductance values. Another factor to consider is that the AMIE model does use a solar-induced conductance model, which perhaps is incorrectly accounting for the change of seasons. Both of these possibilities should be investigated. As with the other cases, the strong differences can be explained two ways. Clearly, because of the seasonal dependence of the O^+/H^+ mixing ratio, the DMSP data will see some effect. It is possible remnants of this effect are present in the winter data even after filtering with the RPA. One could conceivably develop an algorithm to remove

Table 2. Percentage of DMSP Orbits Which Match the AMIE Data According to the Criteria Defined in the Results Section^a

| Satellite | All Data | 2000 Data Only | Summer Only | AL < -400 |
|-----------|----------|----------------|-------------|-----------|
| F-12 | 9.7% | 10.6% | 12.7% | 6.8% |
| F-13 | 35.4% | 35.6% | 40.4% | 55.5% |
| F-14 | 8.9% | NA | 9.7% | 15.6% |
| F-15 | 7.1% | 9.0% | 9.2% | 9.3% |

^aThe column heading lists the subset of the data examined.

this trend from the data possibly using the AMIE data as a comparison data set.

[30] The lack of a strong correlation with activity level is slightly surprising. We had expected improvement because at higher activity levels as the auroral oval is pushed lower and takes a more definite shape giving few “skimmer” passes where the satellite does not fully sample the oval. In experiments where we looked only at orbits where the maximum MLAT obtained by the DMSP spacecraft was greater than 80, we noted significant improvement in the DMSP-AMIE correlation. A possible explanation for the discrepancy is that the more active oval is changing rapidly on time scales AMIE does not reflect, thereby counteracting the effects of the better DMSP sample.

[31] One of the most important questions we face in this study is why are such a large percentage of the runs failing to match, even given the fairly liberal criteria as described in the preface to Table 2? One obvious answer is that the electric field in the auroral zone is highly variable over very short timescales. In the work of Matsuo *et al.* [2003] they found that the electric field is highly variable and dependant on MLT and season which are relevant to our study. So, even though we have AMIE runs at a high cadence (1.0 min), there may be significant changes intrasample detected by DMSP’s 4-s sample rate but not AMIE. This effect should be minimized by our filtering criteria and smoothing and certainly does not account for all of the large difference between the two. Another explanation for some passes at least is shown in Figure 9.

[32] Here (in Figure 9a) we observe that despite very good northern hemisphere station coverage there are cases where the track passes through with little or no observed data directly below. In that case, AMIE is presenting a mix of empirical models [Weimer, 1996] and observation which Bekerat *et al.* [2003] have already established as inadequate for describing the instantaneous convection pattern. In Figure 9b we see that even when there is reasonable coverage on the majority of the pass, the main flow peaks can still be off in both magnitude and location. The very significant falloff for matches in the noon-midnight spacecraft is interesting in that it is not primarily driven by the AT-PCP difference. That is to say, if we relax the success criteria to say allow for 100% variance in the observed cross polar cap potential, we still only get a match 12% of the time for F-12. This means the two are not in agreement in the location of the flows in addition to the magnitude. By going back further in time to another dawn-dusk DMSP satellite, it should be possible to determine if this is a characteristic of spacecraft or orbit. One factor that leads us to suspect it may be a property of the orbit is evident in Figure 4. Here we see that the noon-midnight satellites all have proportionally less data make it through the filtering process than does F-13. In fact, in the final step of the filter, checking that the potential returns to zero, F-13 passes 31%

Table 3. Average AT-PCP, kV, Binned by Spacecraft and Season

| Season | F-12 | F-13 | AMIE (F-13 Track) |
|--------|------|------|-------------------|
| Spring | 36.6 | 40.5 | 33.3 |
| Summer | 38.5 | 40.4 | 34.3 |
| Fall | 37.9 | 40.3 | 34.3 |
| Winter | 41.9 | 44.7 | 30.6 |

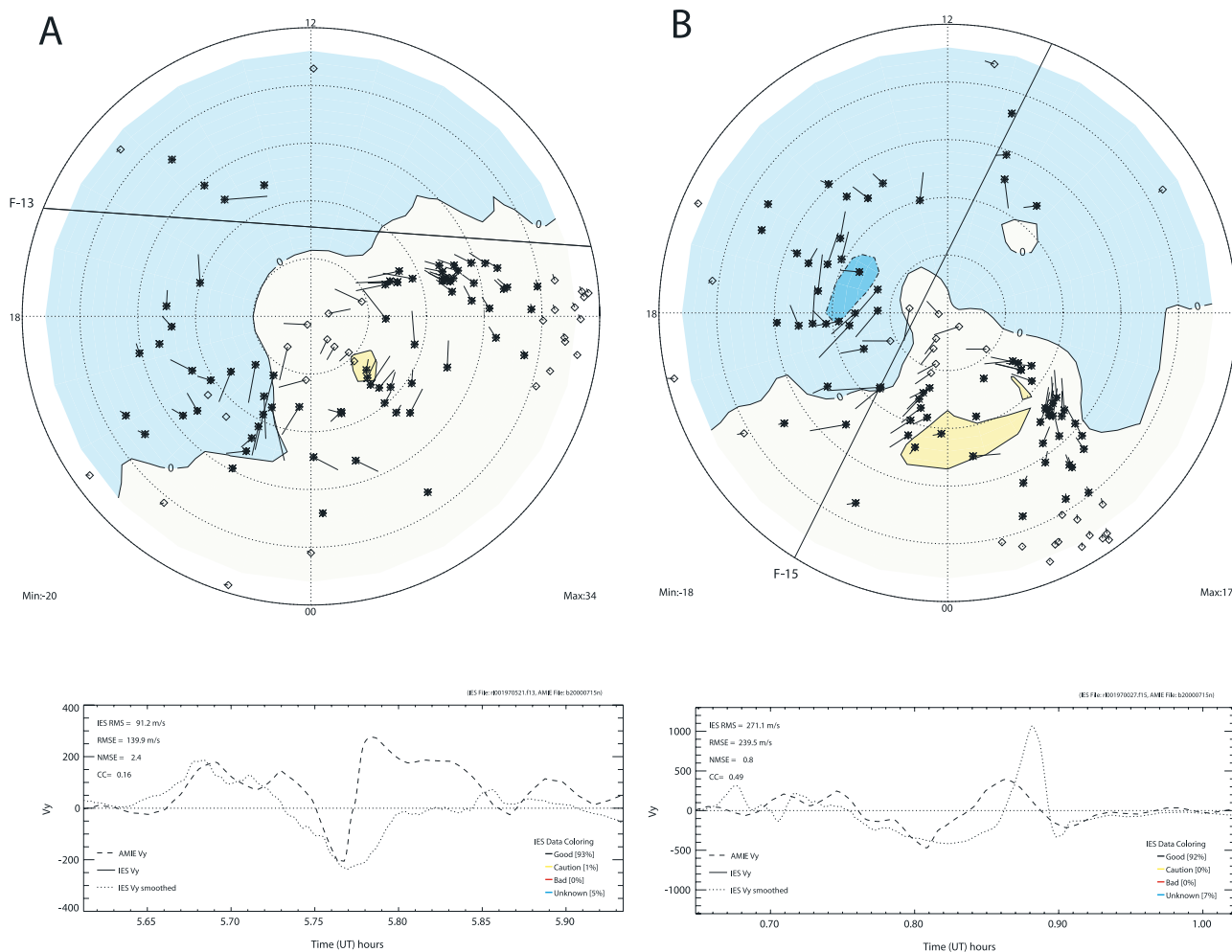


Figure 9. A and B show DMSP passes (solid line) through a corresponding AMIE potential pattern with diamonds representing ground stations used in the calculation. The bottom panel shows a comparison of the AMIE and DMSP V_ys as in Figure 3.

of the time, where F-12 is less than 15%, F-14 less than 10%, and F-15 less than 12%. This leads us to believe that whatever is causing the failure is leaving some sort of a bias in the data even in those passes marked good. The fact that we see some improvement with season and year is evidence that the O⁺/H⁺ mixing ratio plays a part, but again restricting the sample to only summer around solar max does not produce as good a correlation as with F-13. A large part of this could be attributed to the variability in the 18–23 MLT sector as compared to those sectors in F-13's orbit.

6. Summary and Conclusions

[33] Describing the high-latitude convection patterns is very important in many domains including the ionosphere, thermosphere, and magnetosphere. More and more of these applications are being transitioned to near-real time support and the convection pattern is used as a key input allowing for accurate forecast and specification of a given domain. Because of the strongly variable nature of the high-latitude ionosphere, the current best approach for describing it seems to be the use of data assimilation models like AMIE but it is important to understand how well the output of these techniques corresponds with observational data.

[34] In this paper we have compared the ion drift velocities and electric field derived from the AMIE data assimilation model using primarily ground magnetometer input with the same parameters observed by DMSP's SSIES instrument. We have binned the results according to various criteria, including satellite, year, season, and activity level and find significant differences among them. While the study does not attempt to validate the results of either model or data, it does raise some interesting questions with respect to their use and stability. We find that the best correlation between model and data is between F-13 and AMIE. It is not clear if this is a property of the orbit, which is unique in this study, or the instrument. When we apply a set of evaluation criteria for successfully matching over an orbit, we find that F-13 matches the AMIE result between 35% and 55% of the time depending on the criteria mentioned above. We find that the other satellites have a self-similar and much lower correlation ranging from 7% to 13%. The spacecraft in the noon-midnight orbit do correlate well with each other, which implies the instruments are similarly calibrated. While not directly comparable, it is interesting to note that *Bekerat et al.* [2003] using their criteria obtained a result for the empirical *Weimer* [2001] model of 6–17% using F-13 only.

[35] The most significant result from our data is that the AMIE calculated AT-PCP is low compared with DMSP observations. We also find that season is a strong influence across all spacecraft. The summer data correlates much better with AMIE than the winter data, which may be attributed to AMIE's background conductance. The criteria of year, reflecting the changing solar cycle, is a strong influence on the noon-midnight spacecraft, while showing no significant effect for the F-13 spacecraft which is in a dawn-dusk orbit. We attribute a large percentage of this effect to residuals left in the DMSP data but allow that parts of the AMIE model contribute as well.

[36] **Acknowledgments.** Research at the University of Michigan was supported by NSF grant ATM-9802149. We are grateful to the following groups for providing magnetometer data crucial to our AMIE runs: CANOPUS (Canadian Space Agency), IMAGE (Finnish Meteorological Institute), MEASURE (University of California Los Angeles), Greenland coastal chains (Danish Meteorological Institute), MAGIC (University of Michigan), MACCS (Augsburg and Boston University), 210 magnetic meridian (Kyushu University and Nagoya University), and INTERMAGNET.

[37] Arthur Richmond thanks Vladimir Papitashvili and Daniel R. Weimer for their assistance in evaluating this paper.

References

- Ahn, B.-H., A. Richmond, Y. Kamide, H. Kroehl, B. Emery, O. de la Beaujardière, and S.-I. Akasofu (1998), An ionospheric conductance model based on ground magnetic disturbance data, *J. Geophys. Res.*, *103*, 14,769.
- Bekerat, H. A., R. W. Schunk, and L. Scherliess (2003), Evaluation of statistical convection patterns for real-time ionospheric specifications and forecasts, *J. Geophys. Res.*, *108*(A12), 1413, doi:10.1029/2003JA009945.
- Casdagli, M. (1989), Nonlinear prediction of a chaotic time series, *Physica D*, *35*, 335.
- de la Beaujardiere, O., D. Alcayde, J. Fontanari, and C. Leger (1991), Seasonal dependence of high-latitude electric fields, *J. Geophys. Res.*, *96*, 5723.
- Dremukhina, L., A. Levitin, and V. Papitashvili (1998), Analytical representation of the izmeem model for near-real time prediction of electromagnetic weather, *J. Atmos. Sol. Terr. Phys.*, *60*, 1517.
- Fuller-Rowell, T., and D. Evans (1987), Height-integrated Pedersen and Hall conductivity patterns inferred from TIROS-NOAA satellite data, *J. Geophys. Res.*, *92*, 7606.
- Heppner, J., and N. Maynard (1987), Empirical high-latitude electric field models, *J. Geophys. Res.*, *92*, 4467.
- Kamide, Y., A. Richmond, and S. Matsushita (1981), Estimation of ionospheric electric fields, ionospheric currents, and field-aligned currents from ground magnetic records, *J. Geophys. Res.*, *86*, 801.
- Kihn, E. A., and A. J. Ridley (2005), A statistical analysis of the assimilative mapping of ionospheric electrodynamics auroral specification, *J. Geophys. Res.*, *110*, A07305, doi:10.1029/2003JA010371.
- Kustov, A., et al. (1997), Dayside ionospheric plasma convection, electric fields, and field-aligned currents derived from the superdarn radar observation and predicted by the izmeem model, *J. Geophys. Res.*, *102*, 24,057.
- Lu, G., et al. (1996), High-latitude ionospheric electrodynamics as determined by the assimilative mapping of ionospheric electrodynamics procedure for the conjunctive SUNDIAL/ATLAS 1/GEM period of March 28–29, 1992, *J. Geophys. Res.*, *101*, 26,697.
- Matsuo, T., A. Richmond, and K. Hensel (2003), High-latitude ionospheric electric field variability and electric potential derived from DE-2 plasma drift measurements: Dependence on IMF and dipole tilt, *J. Geophys. Res.*, *108*(A1), 1005, doi:10.1029/2002JA009429.
- Papitashvili, V., and F. Rich (2002), High-latitude ionospheric convection models derived from DMSP ion drift observations and parameterized by the IMF strength and direction, *J. Geophys. Res.*, *107*(A8), 1198, doi:10.1029/2001JA000264.
- Papitashvili, V., B. Belov, D. Faermark, Y. Feldstein, S. Golyshev, L. Gromova, and A. Levitin (1994), Electric potential patterns in the northern and southern polar regions parameterized by the interplanetary magnetic field, *J. Geophys. Res.*, *99*, 13,251.
- Papitashvili, V., F. Rich, M. Heinemann, and M. Hairston (1999), Parameterization of the defense meteorological satellite program ionospheric electrostatic potentials by the interplanetary magnetic field strength and direction, *J. Geophys. Res.*, *104*, 177.
- Rich, F., and M. Hairston (1994), Large-scale convection patterns observed by DMSP, *J. Geophys. Res.*, *99*, 3827.
- Richmond, A. (1992), Assimilative mapping of ionospheric electrodynamics, *Adv. Space Res.*, *12*, 59.
- Ridley, A., and E. Kihn (2004), Polar cap index comparisons with AMIE cross polar cap potential, electric field, and polar cap area, *Geophys. Res. Lett.*, *31*, L07801, doi:10.1029/2003GL019113.
- Ridley, A., G. Crowley, and C. Freitas (2000), A statistical model of the ionospheric electric potential, *Geophys. Res. Lett.*, *27*, 3675.
- Weimer, D. (1996), A flexible, IMF dependent model of high-latitude electric potential having "space weather" applications, *Geophys. Res. Lett.*, *23*, 2549.
- Weimer, D. (2001), An improved model of ionospheric electric potentials including substorm perturbations and application to the Geospace Environment Modeling November 24, 1996, event, *J. Geophys. Res.*, *106*, 407.
- Winglee, R. M., V. O. Papitashvili, and D. R. Weimer (1997), Comparison of the high-latitude ionospheric electrodynamic inferred from global simulation and semiempirical models for the January 1992 GEM campaign, *J. Geophys. Res.*, *102*, 26,961.

M. R. Hairston, William B. Hanson Center for Space Sciences, University of Texas at Dallas, P. O. Box 830688, MS WT15, Richardson, TX 75083-0688, USA.

E. A. Kihn and R. Redmon, National Geophysical Data Center, NOAA, 325 Broadway, Boulder, CO 80305, USA. (eric.a.kihn@noaa.gov)

A. J. Ridley, Center for Space Environment Modeling, University of Michigan, 1517 Space Research Building, Ann Arbor, MI 48109-2143, USA.